# INTERNATIONAL SOCIETY FOR SOIL MECHANICS AND GEOTECHNICAL ENGINEERING



This paper was downloaded from the Online Library of the International Society for Soil Mechanics and Geotechnical Engineering (ISSMGE). The library is available here:

## https://www.issmge.org/publications/online-library

This is an open-access database that archives thousands of papers published under the Auspices of the ISSMGE and maintained by the Innovation and Development Committee of ISSMGE.

The paper was published in the proceedings of the 20<sup>th</sup> International Conference on Soil Mechanics and Geotechnical Engineering and was edited by Mizanur Rahman and Mark Jaksa. The conference was held from May 1<sup>st</sup> to May 5<sup>th</sup> 2022 in Sydney, Australia.

# Chemo-mechanical models for acidizing assisted hydro-fracturing

Modèles chimio-mécaniques pour l'hydrofracturing assistée par acidification

#### ManMan Hu & XiaoJie Tang

Department of Civil Engineering, The University of Hong Kong, Hong Kong, mmhu@hku.hk

ABSTRACT: The technique of hydro-fracturing, together with horizontal drilling, has been widely used in many countries for the extraction of subsurface energy in the form of e.g. hydrocarbon and heat. For unconventional tight carbonate reservoirs, characterized by ultralow intrinsic permeability, acidizing treatment is often incorporated as an enhancement of crack propagation. Acidizing assisted hydro-fracturing, during or after the treatment phase, is a highly nonlinear coupled dynamic process that involves several physical/chemical processes occurring concurrently and affecting each other. We are particularly interested in the modelling of crack propagation into a stressed medium subject to fluid pressurization and meanwhile being affected by the chemically aggressive environment. This presentation shows our unique approach of tackling this problem by considering the effect of micro-fracturing enhanced chemical shrinkage, in both the normally defined elastic and plastic domains of the rock behaviour. Local reactive diffusion processes are coupled with the mechanical degradation via upscaling to a representative elementary volume. To this end, a general framework of reactive chemo-elasto-plasticity is formulated, based on which, boundary value problems simulating typical scenarios encountered in hydraulic fracturing will be investigated, with an emphasis on the feedback mechanisms between the coupled processes and the evolution of permeability.

RÉSUMÉ: La technique de l'hydrofracturing, associée au forage horizontal, a été largement utilisée dans de nombreux pays pour l'extraction d'énergie souterraine sous la forme de p. hydrocarbure et chaleur. Pour ces réservoirs de carbonate étanches non conventionnels, caractérisés par une faible perméabilité, un traitement acidifiant est souvent incorporé pour améliorer la propagation des fissures. L'acidification de l'hydrofracturing assistée, pendant ou après la phase de traitement, est un processus dynamique couplé hautement non linéaire qui implique plusieurs processus physiques/chimiques se produisant simultanément et s'influençant mutuellement. Nous nous intéressons particulièrement à la modélisation de la propagation des fissures dans un milieu sollicité soumis à la pressurisation du fluide et étant quant à lui affecté par l'environnement chimiquement agressif. Cette présentation montre notre approche unique pour aborder ce problème en considérant l'effet du rétrécissement chimique amélioré par micro-fracturing, à la fois dans les domaines élastique et plastique normalement définis du comportement de la roche. Les processus de diffusion réactive locale sont couplés à la dégradation mécanique par mise à l'échelle à un volume élémentaire représentatif. À cette fin, un cadre général de chimio-élasto-plasticité réactive est formulé, à partir duquel seront étudiés des problèmes de valeurs limites simulant des scénarios typiques rencontrés en fracturing hydraulique, en mettant l'accent sur les mécanismes de rétroaction entre les processus couplés et perméabilité.

KEYWORDS: chemo-mechanics, acidizing, reactive-diffusion, micro-fracturing, solid-fluid interface.

#### 1 INTRODUCTION

Since the development of horizontal drilling, the technique of hydro-fracturing has been widely used all over the world in the past a few decades for efficient extraction of geo-energy, mainly in the form of hydrocarbon and heat. The extraordinary boom in unconventional shale gas exploration in the United States has spurred interest in exploring for shale gas in other countries. However, these unconventional resources usually locate in very tight low-permeability formations, making a commercial production rate very difficult to meet with conventional methods (Chabora et al. 2012; Rahman 2008). Consequently, the idea of incorporating acidizing as a pretreatment became plausible as acid is known for lowering material toughness or damage tolerance of the rock formation facilitating generation of cracks. Acidizing assisted hydrofracturing has hence emerged as a desirable well stimulation technique owing to its advantages in efficiently creating pathways in unconventional reservoirs, particularly in lowpermeability carbonate-rich reservoirs. However, proper modelling of the multiphysics multiscale processes involved is still outstanding. Field applications without in-depth understanding of the fundamental coupled chemo-mechanical interactions have resulted in unnecessary commercial costs as well as serious environmental concerns.

Reactive chemo-mechanical models have been previously proposed to describe the effects that a chemically aggressive environment may exert on the mechanical behaviour of a geomaterial, involving internal deterioration, mineral mass redistribution and the coupling to the stress field, and hence material compliance and strength (e.g. Hu and Hueckel 2013; Loret et al. 2002; Hueckel 1997). In this short paper, a generic framework of reactive chemo-elasto-plasticity is presented as a first-step approach to tackle the complex problem of acidizing assisted hydro-fracturing. In our particular formulation, the effect of micro-fracturing enhanced chemical shrinkage is considered, in both the normally defined elastic and plastic domains of the rock behaviour. Local reactive diffusion processes are coupled to the time-dependent process of material degradation via a meso-scale conceptualization of a representative elementary volume (REV).

In what follows, we present the constitutive formulation of our fully coupled chemo-hydro-geomechanical model followed by a brief outline of the numerical implementation strategy, which is conducted in an open-source Finite Element simulator based on the Multiphysics Object Oriented Simulation Environment (MOOSE). Subsequently, we present case studies focusing on a two-dimensional cracking scenario with the crack surface subject to fluid pressurization and acidizing concurrently.

## 2 REACTIVE-CHEMO-MECHANICAL MODEL

# 2.1 Reactive-chemo-elasticity and reactive-chemo-plasticity

As for a geomaterial subject to chemical degradation, the total strain rate can be decomposed into the elastic and plastic components:

$$\dot{\varepsilon}_{ij} = \dot{\varepsilon}_{ij}^{el} + \dot{\varepsilon}_{ij}^{pl} \tag{1}$$

The chemical effect is assumed to play a role on both the elastic and the plastic parts (Hu and Hueckel 2013). Elastic (reversible) component is described in Eq. (2) in which  $\sigma_{ij}$  denotes the stress tensor. The elasticity tensor  $E_{ijkl}$  is here expressed as a function of a scalar variable  $\xi^{loc}$  which represents the time integration of local mineral mass removal, that is, at a chemical length scale within the REV (Hu and Hueckel 2019).

$$\sigma_{ij} = E_{ijkl}(\xi^{loc}) \cdot \varepsilon_{kl}^{el}$$
 (2a)

$$\xi^{loc} = \int_0^t \dot{\xi}^{loc} d\tau \tag{2b}$$

The irreversible plastic strain rate is assumed to be described by an associated flow rule:

$$\dot{\varepsilon}_{ij}^{pl} = \dot{\lambda} \frac{\partial f}{\partial \sigma_{ii}} \tag{3}$$

Where  $\frac{\partial f}{\partial \sigma_{ij}}$  denotes the yield locus gradient which

determines the mode of plastic strain rate, and  $\lambda$  is a multiplier function referring to the rate magnitude expressed as:

$$\dot{\lambda} = \sqrt{\dot{\varepsilon}_q^{pl^2} + \dot{\varepsilon}_v^{pl^2}} \tag{4}$$

Where  $\dot{\varepsilon}_q^{pl}$  and  $\dot{\varepsilon}_v^{pl}$  represent the deviatoric and volumetric invariants of the plastic strain rate, respectively, following the Perzyna's overstress model (Perzyna 1966):

$$\begin{cases} \dot{\varepsilon}_{q}^{pl} = \dot{\varepsilon}_{0} \left( \frac{q - q\gamma}{\sigma_{ref}} \right)^{m} \\ \dot{\varepsilon}_{v}^{pl} = \dot{\varepsilon}_{0} \left( \frac{p' - p\gamma}{\sigma_{ref}} \right)^{m} \end{cases}$$
 (5)

Where  $\dot{\varepsilon}_0$  is a reference strain rate, q and p' denoting the equivalent deviatoric stress and the volumetric mean effective stress, respectively.  $\langle \cdot \rangle$  represents the Macaulay brackets.  $q_Y$  and  $p_Y$  indicate the deviatoric and normal components of the yield stress, respectively. m is the exponent in the power law stress-strain relationship.

To quantitatively describe the evolution of mechanical properties during the chemical processes, we use  $\xi^{REV}$ , i.e. the accumulated mass removal at REV-scale, to link to the continuum behaviour of the rock, which is mathematically expressed as:

$$\begin{cases} q_Y = q_{Y_0} (1 - \beta_q \xi^{REV}) \\ p_Y = p_{Y_0} (1 - \beta_p \xi^{REV}) \end{cases}$$
 (6)

Where  $q_{Y0}$  and  $p_{Y0}$  are the deviatoric and normal components of the initial yield stress without chemical degradation.  $\beta_p$  and  $\beta_q$  are constant coefficients indicating the weakening effect on the deviatoric and normal yield stress

components, respectively.

Regarding a specific rock material,  $\xi_n$  (n=1,2,...) can be used to represent the accumulated dissolved mass of the n-th species of mineral within the REV (Hu and Hueckel 2013). Here we consider a carbonate-rich rock and hence simplify the dissolved mineral to be calcite only. Note that  $\xi^{REV}$  represents the fraction of the dissolved portion over the total soluble mass in the solid matrix, suggesting that at extreme conditions its value can approach unity. Note also that  $\xi^{REV}$  is a REV-averaged variable, denoting the integrated mass removal of a local mineral dissolution rate  $\dot{\xi}^{loc}$  overtime, which is directly linked to the microcracking process owning to its characteristic generation rate of specific surface area (Hueckel and Hu 2009; Ciantia and Hueckel 2013) as expressed in the following equation:

$$\xi^{REV} = \int_0^t (1 + \eta \hat{\varepsilon}) \dot{\xi}^{loc} d\tau \tag{7}$$

where  $\hat{\varepsilon}$  denotes a strain invariant, acting as a proxy for local mechanical damage.  $\eta$  denotes the coefficient of microfracturing enhancement on the process of chemical dissolution.

# 2.2 Reactive-transport of solute coupled with hydrogen diffusion

Carbonate-rich rocks, e.g. limestones and dolostones, are susceptible to degradation when subject to an acidic environment, where both mechanical and chemical processes may take place. Here, we consider a weak acidic condition for a carbonate-rich rock under which acid diffusion and the dissolution of calcium carbonate occur at comparable time-scales. The chemical process is assumed to be dominated by the following reaction:

$$CaCO_3(s) + H^+(aq) \leftrightarrow Ca^{2+}(aq) + HCO_3^-(aq)$$
 (8)

Under such condition, the rate at which calcium carbonate dissociates into the solution depends on the local hydrogen concentration in the fluid phase (Sjöberg and Rickard, 1984). Accordingly, the rate of calcium mass removal from the solid phase, as well as the change rate of Ca<sup>2+</sup> concentration in pore water is assumed to follow a power law function of local hydrogen concentration, resulting in the reaction-transport process of Ca<sup>2+</sup> being coupled to the deformation/damage of the solid matrix. Based on it, solute transport is assumed to be described by a reactive diffusion equation with a nonlinear source term as illustrated below:

$$\partial_t x_{Ca^{2+}} = D_{Ca^{2+}} \nabla^2 x_{Ca^{2+}} + \beta_{H^+} (1 + \eta \hat{\varepsilon}) (C_{H^+})^{k'}$$
 (9)

where  $x_{Ca^{2+}}$  denotes the molar fraction of calcium in the fluid phase within the process zone,  $D_{Ca^{2+}}$  denoting the diffusivity of calcium, assumed as constant in the process zone.  $\beta_{H^+}$  denotes a lumped constant representing a combined effect of local acidity and damage enhancement on the mass dissolution rate. The exponent k' is usually assumed as constant with a value between  $0.5\sim1.0$  (Sjöberg 1976). The evolution of acidity distribution over time is controlled by

$$\partial_t C_{H^+} = D_{H^+} \nabla^2 C_{H^+} - \gamma_{CH} \dot{\xi}^{REV} \tag{10}$$

Where  $C_{H^+}$  indicates the local concentration of hydrogen,  $D_{H^+}$  denoting the diffusivity of hydrogen.  $\gamma_{CH}$  is a proportionality constant of the mass exchange rate of hydrogen consumption over that of calcium production in the fluid phase.

# 3 NUMERICAL IMPLEMENTATION AND MODELLING ESTABLISHMENT

The proposed chemo-mechanical model has been implemented in an open-source FEM simulator built on the multiphysics multiscale platform MOOSE (Gaston et al. 2009; Poulet et al. 2017; Poulet and Veveakis 2016), which allows for high-performance computing in a tightly coupled manner. A group of dimensionless variables are required in the final set of governing equations to facilitate computation. Variables covered in the current contribution are normalized following the transformation below

$$x^{\star} = \frac{x}{L_{ref}}, \ \sigma^{\star}_{ij} = \frac{\sigma_{ij}}{\sigma_{ref}}, \ C^{\star} = \frac{c}{c_{ref}}, \ t^{\star} = \frac{t}{t_{ref}}$$
 (11)

Where  $L_{ref}$ ,  $\sigma_{ref}$ ,  $C_{ref}$ , and  $t_{ref}$  denotes the reference value of displacement, stress, hydrogen concentration and time,

respectively, and time reference is derived via  $t_{ref} = \frac{L_{ref}^2}{D_{H^+,ref}}$ .

Notably,  $C_{ref}$  in this model represents the concentration in a neutral condition where no chemical reaction occurs accordingly.

In what follows we investigate a two-dimensional crack propagation problem (see Fig. 1) where the crack surface is subject to a constant hydraulic pressure ( $p_a$ ) and an instantaneous long-lasting acidizing exposure ( $C_{H^+|a}$ ), with the exterior boundary under constant overburden pressure ( $p_b$ ). The basic parameters used include b/a=15, E=30 GPa, v=0.25, the initial rock cohesion  $c_0=10$  MPa, slope of the yield surface  $\mu=0$ ,  $D_{H^+}=3.6\times 10^{-5}$  cm²/s (Fredd and Fogler 1998),  $p_a=0.4$  MPa,  $p_b=0$ .  $C_{H^+|a}$  exposed on the crack surface represents a weak acid condition of pH 5.3.

The chemical processes related parameters used in this study are  $\beta_p = 0$ ,  $\beta_q = 1$ ,  $\eta = 2 \times 10^4$  (Hu and Hueckel 2013), k' = 0.9,  $\beta_{H^+} = 2.5 \times 10^{-3}$  (Ciantia et al. 2015) unless any of them is a subject of a parametric study. Notably, local mechanical damage  $\hat{\varepsilon}$  is represented by the irreversible deviatoric strain invariant which evolves during the process.

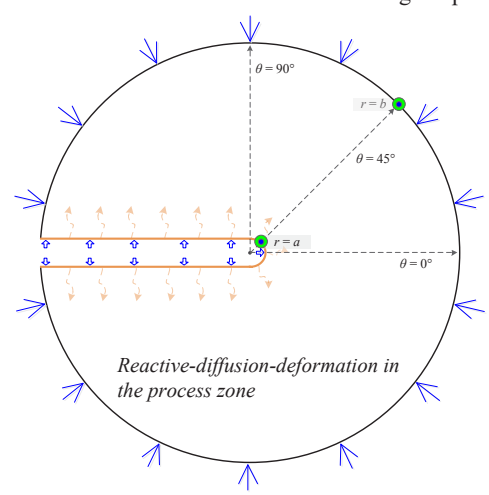


Figure 1. Acidizing assisted hydro-fracturing model (of a single fracture) in the presence of hydrogen infiltration. The crack surface is subject to constant hydraulic pressure and acidizing, and the outer boundary is constrained by overburden pressure.

#### 4 SIMULATION RESULTS

Our simulation results show that the distribution of hydrogen concentration along the radius at the crack propagating direction undergoes a significant evolution, particularly in the first few days (e.g. from the beginning of exposure to 200 hours). As depicted in Fig. 2, after 500 hours of acidic treatment, the acidity distribution is in an approximately steady-state after which the pH value barely changes, suggesting a uniform local reaction rate  $\dot{\xi}^{loc}$  within the process zone.

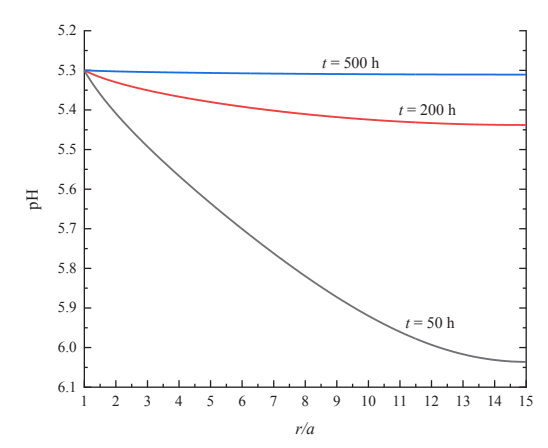


Figure 2. Evolution of the distribution of acidity (represented by the pH values) along the radius at propagation direction ( $\theta = 0^{\circ}$ ), upon 50, 200 and 500 hours of exposure of the combined action of acidizing and pressurization.

Fig. 3 shows the distribution of the deviatoric stress invariant along the radius at  $\theta=0^{\circ}$ . The maximum value of each distribution curve (better shown in the magnified view) defines the location of the moving elasto-plastic interface. The q value within the plasticity range undergoes a noticeable decrease owing to its higher concentrated acid infiltration as well as the acceleration in induced damage (represented by irreversible deviatoric strain). As the reaction continues, the immediately adjacent exterior area yields into a plasticity state. This progressive material yielding is chemically driven and hence controlled by the reaction-diffusion processes.

Inside the chemo-plasticity zone, the yield limit at each material point drops dramatically throughout the acidizing process. As illustrated in Fig. 3, at four increased timesteps, namely t=0, 300h, 600h and 900h, the deviatoric strength at the crack tip point exhibits the value of  $c_0$ ,  $0.936c_0$ ,  $0.819c_0$  and  $0.577c_0$ . Meanwhile, the value of corresponding accumulated mass removal at the crack tip is 0, 0.064, 0.181 and 0.423, respectively, indicating a nonlinear relationship between strength loss and the chemical mass removal processes. Also, as depicted by the contour map of the deviatoric strain invariant around the crack tip shown in Fig. 4, the regional mass removal starts to increase exponentially when localized damage emerges at the tip area, which is an expected result of damage-dissolution coupling.

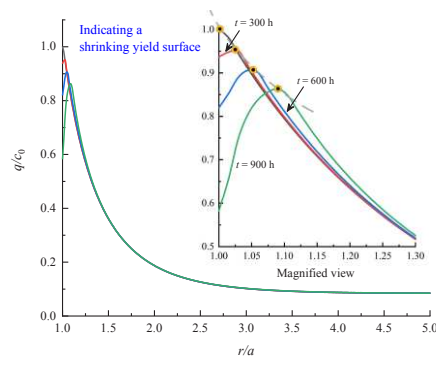


Figure 3. Evolution of the distribution of deviatoric stress normalized by the initial cohesion along the radius at propagation direction ( $\theta = 0^{\circ}$ ), upon 300, 600 and 900 hours of exposure.

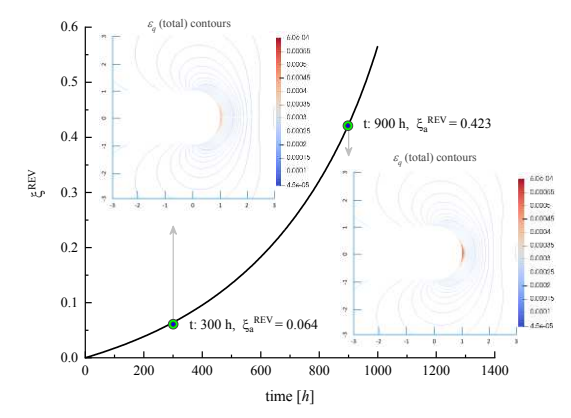


Figure 4. Evolution of the accumulated mass removal at crack tip subject to long-lasting acid exposure of pH 5.3. The contours of the deviatoric strain suggest an emergence of localized damage at the tip region, accelerating mineral dissolution, under the combined action of acidizing and pressurization.

The distribution of the deviatoric stress invariant along the radius at  $\theta=0^\circ$ ,  $45^\circ$ ,  $90^\circ$  upon 900 hours of chemical exposure is demonstrated, respectively, in Fig. 5. At  $\theta=0^\circ$ , a localized area of chemical yielding at the tip is prominent, while no significant yielding is observed at  $\theta=45^\circ$  and  $\theta=90^\circ$ . Therefore, the deviatoric stress distribution at  $\theta=45^\circ$  and  $\theta=90^\circ$  decreases monotonically from the crack tip area towards the exterior boundary. Fig. 5 also indicates that the region between  $\theta=-45^\circ$  and  $\theta=45^\circ$  around the crack tip is the area affected most by the two-way coupling of chemical and mechanical processes, and hence the location where multiscale multiphysics instabilities may occur.

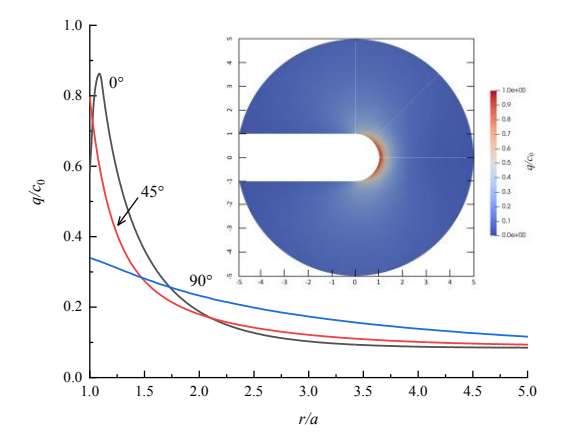


Figure 5. The distribution of deviatoric stress normalized by the initial cohesion along the radius of rays at  $\theta = 0^{\circ}, 45^{\circ}, 90^{\circ}$  upon 900 hours of exposure.

In what follows we perform a sensitivity study on the role that micro-fracturing intensity plays on the crack propagation. Fig. 6 shows the evolution of the displacement of the crack tip point under various values of the coupling coefficient,  $\eta$ , representing the effect of the microcracking enhancement on the chemical dissolution process. For the case of  $\eta=0$ , i.e. one-way coupling, the displacement of the crack tip exhibits a mild degree of nonlinearity, due to the lack of feedbacks from the mechanical process to the reaction-diffusion processes. For  $\eta=1\times10^4$ , as the reaction progresses, the crack propagation shows an exponential development over time. When the microfracturing coefficient is doubled, i.e.  $\eta=2\times10^4$  (meaning the material more susceptible to microcracking), the crack tip propagation demonstrates a substantial increase in terms of the displacement and its rate. The acceleration clearly results from

the mutually promoting feedbacks of chemical mass removal and material degradation in the evolving complex system.

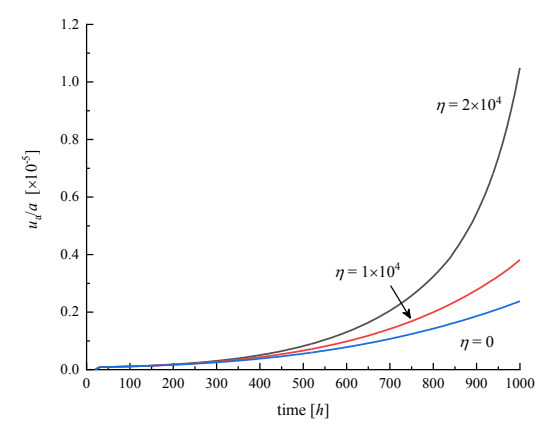


Figure 6. Displacement of the crack tip point (representing crack propagation) normalized with a over time, for the one-way ( $\eta = 0$ ) and two-way ( $\eta = 1 \times 10^4$ ,  $2 \times 10^4$ ) couplings.

The stress intensity factor (SIF) is frequently used in the fracture mechanics community for making sensible prediction of stress state and material toughness. Mode I (tensile) crack SIF can be derived via calculating the J-integral around the crack tip, so that the crack tip singularity can be conveniently avoided. In our current model, the singularity is instead smoothened by assuming a blunt crack tip. Fig. 7 shows the time evolution of the mode I SIF among cases characterized by various microcracking enhancement,  $\eta$ . For the one-way coupling case ( $\eta = 0$ ), the SIF evolves exponentially as the crack tip propagates (see Fig. 6). It is interesting to note from Fig. 7 that when  $\eta$  is increased by the same interval of  $1 \times 10^4$ , the increase in induced stress intensity factor at a given time is more or less equal.

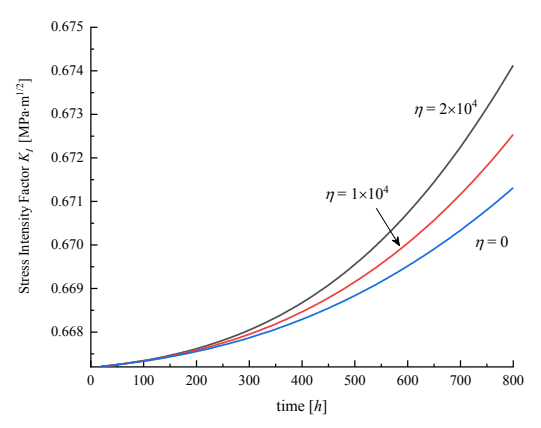


Figure 7. Evolution of the mode I stress intensity factor for the one-way ( $\eta = 0$ ) and two-way ( $\eta = 1 \times 10^4$ ,  $2 \times 10^4$ ) couplings.

### 5 CONCLUSIONS

In this short paper, we presented a chemo-mechanical model for acidizing assisted hydro-fracturing considering both the elastic and plastic domain of the rock behaviour. The constitutive framework was formulated based on cross-scale coupling of material degradation and associated reactive diffusion processes. Subsequently, numerical investigation of a two-dimensional cracking scenario subject to combined action of fluid pressurization and an instantaneous long-lasting acid exposure was performed. The numerical results show that chemical dissolution (together with the dissipative diffusion) plays a crucial role throughout the cracking process in terms of

the redistribution of the stress and deformation field around the crack tip as well as the nonlinear propagation of the crack itself. Subcritical cracking can be chemically driven. The more susceptible the rock is to microcracking under stress, the more accelerated a hydro-fracture propagates.

#### 6 REFERENCES

- Chabora, E., Zemach, E., Spielman, P., Drakos, P., Hickman, S., Lutz, S., Boyle, K., Falconer, A., Robertson-Tait, A., Davatzes, N.C. 2012. Hydraulic stimulation of well 27-15, Desert Peak geothermal field, Nevada, USA. Proceedings of thirty-seventh workshop on geothermal reservoir engineering, Stanford University, Stanford,
- Ciantia, M.O., Castellanza, R., di Prisco, C. 2015. Experimental Study on the Water-Induced Weakening of Calcarenites. *Rock Mechanics* and Rock Engineering. 48(2), 441-461.
- Ciantia, M.O., Hueckel, T. 2013. Weathering of submerged stressed calcarenites: chemo-mechanical coupling mechanisms. *Géotechnique*. 63(9), 768-785.
- Fredd, C.N., Fogler, H.S. 1998. Influence of transport and reaction on wormhole formation in porous media. AIChE journal. 44(9), 1933-1949.
- Gaston, D., Newman, C., Hansen, G., Lebrun-Grandié, D. 2009. MOOSE: A parallel computational framework for coupled systems of nonlinear equations. *Nuclear Engineering and Design*. 239(10), 1768-1778.
- Hu, M.M., Hueckel, T. 2013. Environmentally enhanced crack propagation in a chemically degrading isotropic shale. Géotechnique. 63(4), 313-321.
- Hu, M.M., Hueckel, T. 2019. Modeling of subcritical cracking in acidized carbonate rocks via coupled chemo-elasticity. *Geomechanics for Energy and the Environment*. 19, 100114.
- Hueckel, T. 1997. Chemo-plasticity of clays subjected to stress and flow of a single contaminant. *International journal for numerical and analytical methods in geomechanics*. 21(1), 43-72.
- Hueckel, T., Hu, L.B. 2009. Feedback mechanisms in chemomechanical multi-scale modeling of soil and sediment compaction. *Computers and Geotechnics*. 36(6), 934-943.
- Loret, B., Hueckel, T., Gajo, A. 2002. Chemo-mechanical coupling in saturated porous media: elastic-plastic behaviour of homoionic expansive clays. *International Journal of Solids and Structures*. 39(10), 2773-2806.
- Perzyna, P. 1966. Fundamental Problems in Viscoplasticity. *Advances in Applied Mechanics*. 9, 243-377.
- Poulet, T., Paesold, M., Veveakis, M. 2017. Multi-Physics Modelling of Fault Mechanics Using REDBACK: A Parallel Open-Source Simulator for Tightly Coupled Problems. *Rock Mechanics and Rock Engineering*. 50(3), 733-749.
- Poulet, T., Veveakis, M. 2016. A viscoplastic approach for pore collapse in saturated soft rocks using REDBACK: An open-source parallel simulator for Rock mEchanics with Dissipative feedBACKs. Computers and Geotechnics. 74, 211-221.
- Rahman, M. 2008. Constrained hydraulic fracture optimization improves recovery from low permeable oil reservoirs. *Energy Sources, Part A*. 30(6), 536-551.
- Sjöberg, E.L., Rickard, D.T. 1984. Temperature dependence of calcite dissolution kinetics between 1 and 62°C at pH 2.7 to 8.4 in aqueous solutions. *Geochimica et Cosmochimica Acta*. 48(3), 485-402